Hindawi
Advances in Civil Engineering
Volume 2021, Article ID 5596760, 18 pages
https://doi.org/10.1155/2021/5596760

Research Article

Investigation on Seismic Behavior of Historical Tokatlı Bridge under Near-Fault Earthquakes

Memduh Karalar and Mustafa Yeşil

Zonguldak Bulent Ecevit University, Department of Civil Engineering, Zonguldak, Turkey

Correspondence should be addressed to Memduh Karalar; memduhkaralar@beun.edu.tr

Received 16 February 2021; Revised 16 August 2021; Accepted 27 August 2021; Published 21 September 2021

Academic Editor: Luigi Di Sarno

The main purpose of this study is to compare the static and dynamic behavior of a historical single-span masonry arch bridge under different near-fault earthquakes. The historical Tokatlı Bridge, built in Karabük, is chosen for this study. To investigate the behavior of near-fault earthquakes on the historical masonry bridge, first, a finite element model is built and analyzed under various near-fault earthquakes by using ANSYS and SAP2000. To build a finite element model, 162920 nodes and 47818 elements are used in ANSYS. First, finite element analysis results are compared to each other under Earth gravity. Then, ground motions near the fault are chosen to be used in this study. These earthquakes can be listed as follows: Cape Mend (1992), Kobe (1995), Superstition Hills (1987), Northridge (1994), Imperial Valley (1979), and Chi-Chi (1999). The behavior of the single-span historical bridge is obtained under these ground motions, and the results are compared with each other using contour diagrams using ANSYS. Furthermore, at the end of these analyses, it is observed that the tensile stresses have reached the permissible masonry tensile strength, especially on the upper side of the large belt, on the upper side of the belt, and on the side of the belt, and pose a risk for damage.

1. Introduction

In the past periods where today's engineering facilities and construction materials were not available, it was possible to pass large openings or carry heavy loads with the arch form which is one of the basic elements of the historical bridge design. Arch bridges, which are commonly seen in Turkey, were built in Anatolia, especially in the 19th century by the Ottomans in the form of a single-span stone arch. In Turkey, approximately 1300 of such historical bridges are still in service. It is of the most importance to ensure the safety of these historical bridges against the dynamic loadings of traffic, wind, and earthquakes. This task requires the accurate identification of the dynamic characteristics of these existing bridges [1]. On the other hand, there are about 35,000 masonry arch bridges in service in the UK, about 96% of the 35,000 in-service masonry arch bridges at the time were over 70 years old, and 20% of these inventories were carrying principal roads [2]. Masonry arch bridges, which are in use worldwide, encompass various sizes, styles, and spans, some of which date back to early antiquity. For example, the six-arch stone bridge 30 m in span built around 100 BC is still in existence in Alcantara, Spain [2].

Considering the effect of near-fault earthquakes can be very important, especially for structures that contain various structural parts, such as historical bridges. These effects could be the main subject particularly for the resonance of structure together with the response of acceleration, velocity, displacements, stress distribution, etc. [3]. It is typically recognized that resonance effects and spectral response mainly appear alongside of building height especially for conventional structures rather than complex structures [4, 5]. It is clear that the abovementioned seismic effects still need to be investigated further for structures such as historical masonry bridges. Furthermore, acceleration, velocity, displacements, stress distribution, etc. due to the complex masonry structures also become an important issue under the effects of soil structure interaction [6–9]. Throughout history, human beings have

built bridges in many different methods and forms, from the simplest methods to the modern technology, and extracted unique works. In these bridges, the arch form was widely used. These historical buildings, dating back to the present and have thousands of years of history, have been damaged or destroyed by disasters such as earthquakes, wars, and fires that have occurred in time. Nowadays, a special attention is necessary to existing national road and rail networks. The mainstream of the bridges in the European railway network, in addition to a large part of those in the road system, consists of these masonry bridge structures [10]. When the literature is examined, it will be seen that there are many analytical and experimental studies on historical bridges [11–13]. Besides these studies, Boothby et al. [14] has investigated the behaviors of the filled arch bridges under the vehicle loads experimentally with the method of finite elements. For this purpose, Boothby et al. [14] has examined five different bridges and has analyzed four of these bridges with ANSYS program. The other study is conducted by Hatzigeorgiou et al. [15]. Hatzigeorgiou et al. [15] has modeled historical masonry Arta Bridge with finite elements and have applied linear and nonlinear static and dynamic analysis on the model. In another study by Fanning and Boothby [16], the Griffith Bridge in Dublin, Ireland, has been analyzed with ANSYS program as 3D solid element, and Fanning and Boothby [16] have done an analysis of the models. Fanning and Boothby [16] examined the results of field testing and FE modeling of three masonry arch bridges in their study. Bridges were tested using a reference frame built under the structure and measuring structural displacements with the help of LVDT devices [16]. Furthermore, 3D nonlinear finite element models were analyzed using ANSYS software and found to provide a good prediction of the actual behavior of a wall arch bridge using a reasonable set of material properties. The other study is performed by Frunzio et al. [17]. Frunzio et al. [17], in their three-dimensional FE analysis of a stone masonry arch bridge involving nonlinear material behavior, found that the results of their FE analysis were useful in generating a qualitative map of the intervention areas for restoration. Frunzio et al. [17] also found that this analysis is strongly dependent upon the exactness of mechanical parameters, which are often difficult to evaluate by experimental analyses, especially in cases of monuments and historical buildings. The other study is performed by Toker and Unay [18]. Toker and Unay [18] also studied the mathematical modeling techniques on a prototype model of a common arch bridge under different loading conditions. Bayraktar et al. [19] determined the dynamic characteristics of historical Sinik Bridge and also updated the bridge FE model by adjusting the boundary condition definitions. In the literature, the other study is performed by Brencich and Sabia [20]. Brencich and Sabia [20] studied Tanaro Bridge. In this study, the natural frequencies, mode shapes, and damping ratios of this 18-span masonry construction were identified by dynamic tests. Diamanti et al. [21] used nondestructive ground-penetrating radar (GPR) on masonry arch bridges for monitoring of ring separation. In order to validate and update the analytical results, several laboratory experiments were conducted. Ural et al. [22] have modeled the concrete-filled steel Beichuan Bridge in the ANSYS finite elements program and have performed analytical models and dynamic experimental analyses. Analytical modeling techniques were used to simulate GPR tests, and the analytical models were updated using laboratory experiments. Another study is performed by Aydin and Özkaya [23]. Aydin and Özkaya [23] also investigated the collapse loads of masonry arch bridges and carried out a study to calculate the behavior of single-span masonry arch bridges under certain loads by the static analysis method. Altunisık et al. [24] conducted a detailed research on the comparison of the static and dynamic behavior of historical masonry arch bridges based on different arch curvatures. For this purpose, to determine the static and dynamic behavior of the bridge, the finite element model is used [24]. To show the arch curvature effect, the finite element model is used as 2.86 m–3.76 m for the first arch and 2.64 m–3.54 m for the second arch, respectively. It is reconstructed in 0.10 m increments, taking into account the different arch curvatures. Thus, arch curvature appears to have more impact on the structural response of historic masonry arch bridges [24]. Breccolotti et al. [25] carried out parametric analysis by changing the rise/span ratio of masonry arch bridges and compared the results with finite element modeling. Rovithis and Pitilakis [26] also investigated the 750 m long "De Bosset" Bridge in the Cephalonia Island of Western Greece to design of the rehabilitation measures and assessment of the pre- and postintervention seismic response of the bridge based on detailed in situ and laboratory tests. The efficiency of the bridge retrofitting is also proved by a preliminary performance analysis of the bridge under the recorded ground motion [26]. The other study is performed by Sayin [27]. In this study, linear and nonlinear dynamic analyses of historical Nadir Bridge are assessed by Sayin [27]. For this purpose, the bridge is modeled with three-dimensional finite elements and then seismic response of the bridge is investigated. As mentioned above, when the literature is searched, it is seen that only a few studies available today are related to the seismic assessment of the historical masonry arch bridge [28–34].

The main objective of this research study is to simulate the performance of historical arch bridge under near-fault earthquakes via finite element (FE) approach and to demonstrate the capability and performance predicting. For this purpose, in this study, the earthquake behaviors of historical arch bridges (historical Tokatlı Bridge) constructed in the Karabuk, Turkey, is investigated. First, the material and geometrical properties of the historical Tokatlı Bridge are described, and then, the FE model of the single-span historical Tokatlı bridge was created and necessary analyzes were carried out. Detailed discussion of the historical arch bridge (historical Tokatlı Bridge) is given in the following sections.

2. Description of the Historical Arch Bridge (Historical Tokatlı Bridge)

The historical Tokatlı Bridge is located on the Söğütlüdere Canyon in the Safranbolu district of Karabük. The bridge is located on the river bed in the east-west axis. The official website of the Karabük Provincial Directorate of Culture and Tourism states that the historical Tokatlı Bridge may have been built in the 18th century. Although there are no

published academic studies on the bridge, the inventory slip prepared by the General Directorate of Highways and the registration voucher prepared by the Ministry of Culture and Tourism are among the few documents providing information about the bridge [35]. A pulley-shaped arch and one-eyed bridge stones were used with smooth fine stones; tempan walls and arch belly were built with small rubble stone technique. While the original stone masonry is seen in the lower parts of the tempan wall, it is seen that the upper levels have been repaired by using stones of different sizes and genders. The bridge is approximately 47.26 meters long and 4.10 meters wide. The height from the bridge to the water level is 30.70 meters. The bridge which extends in the east-west direction continues straight to 33.70 meters in the east direction and then makes a sharp turn to the southeast and continues for 13.56 meters. While the width of the bridge is 4.08 meters at the west entrance, it is expanded to 4.21 meters at the beginning of the turn, narrows to 3.21 meters after the turn, and then extends again to 3.86 meters towards the bridge exit up to the water level of 28.68 m. General view of the historical Tokatlı Bridge is given in Figure 1.

2.1. Finite Element Modeling. In this part of the study, the FE model of the historical Tokatlı Bridge is built and analyzed under various near-fault earthquakes by using the finite element program. For this purpose, first, 3D nonlinear finite element program is generated by using ANSYS [36]. Under various near-fault earthquakes, ANSYS [36] solutions are obtained. Although the finite element method is used as a solution method in both programs, there are differences in the interface of the programs, visuals, creation or definition of models, mesh methods, and the application of loads. In order to see these differences, the finite element model of the historical Tokatlı Bridge model, which has been analyzed in detail with ANSYS program, has been remodeled in SAP2000 [37] program with similar geometry, material information, and support conditions. Then, static and dynamic analyzes are performed. Furthermore, SAP2000 [37] model is also constituted to obtain mode shapes and natural frequencies of the historical Tokatlı Bridge. And then, the results obtained from nonlinear finite element models, ANSYS and SAP2000, are compared. Details of the FE model are described in the following sections.

2.2. Element Types. In the FE modeling of the historical Tokatlı Bridge, the bridge elements are divided into small elements connected at intersecting nodes with degrees of freedom appropriate to the element type selected for modeling of the structure behavior under various loading conditions. The historical Tokatlı Bridge is modeled using 10-node high-order tetrahedron elements. This element model, well suited for modeling irregular networks and contact surfaces, has a quadratic displacement behavior [38]. Accordingly, such an element is suitable for predicting the surface contact between the historical Tokatlı Bridge components and the irregular geometry of the FE model. Every node of the element has three degrees of freedom, that is, translations in the nodal x, y, and z directions. The contact algorithm of the FE model requires the definition of contact surfaces. Details of the contact surface modeling are given in the following section.

2.3. Contact Modeling. Contact mechanics is the study of the deformation caused by solid bodies that touch each other at one or more points [39]. In this study, the contact between the historical Tokatlı Bridge and its components is defined as a surface-to-surface contact type where the contact area may change as a function of the degree of separation of the contact surfaces. This contact type is established when a surface of one body comes in contact with the surface of another body, and it is commonly used for arbitrary bodies that have large contact areas [40, 41]. To define a contact surface pair, one of the surfaces is designated as a contact element and the other as target element. Both elements need to have the same characteristic parameters such as number of nodes and node locations [24]. For the contact interface of the historical Tokatlı Bridge, CONTA174 element and a matching TARGE170 element are used to represent contact and separation between the two surfaces [41], as shown in Figure 2. To facilitate sliding or movement of the fill material relative to the arch barrel and the spandrel walls without generating significant tensile stresses at the interface between these materials, three-dimensional frictional contact surfaces are included [16].

2.4. Meshing. Mesh size and type are important to accurately estimate the stress and/or strain values in a FE model. Thus, to assure an appropriate mesh density in the FE model of the historical Tokatlı Bridge, case studies with different mesh sizes are carried out. Accordingly, four meshing options are tested and compared in the FE model: Automatic, Tetrahedrons, Hex Dominant, and Sweep meshing options, as shown in Figure 3. The first meshing option is an automatically generated mesh, and it consists of 6680 elements and 104788 nodes. The second meshing option, Tetrahedrons mesh, consists of 47818 elements and 162920 nodes. The properties of the other meshing options are shown in Table 1. In ANSYS, a larger number of nodes in a FE model lead to excessive computation time. Therefore, Tetrahedron meshing option as it has a better size distribution and fewer nodes throughout the FE model is selected. The largest mesh size giving stable results is then chosen for the FE model [42, 43]. The maximum strain value in the historical Tokatlı Bridge remains nearly constant for both 50 mm and 25 mm mesh sizes (0.012443 and 0.012466, respectively). Thus, mesh sizes are taken as 25 mm in the contact areas of the model and 50 mm in the rest of the model.

3. Material Model and Boundary Conditions

In the nonlinear FE model, actual material properties of the historical Tokatlı Bridge are needed to achieve accurate analysis results. The material properties used in the analysis of the historical Tokatlı Bridge are listed in Table 2 [19]. In addition to material model, accurate definition of boundary

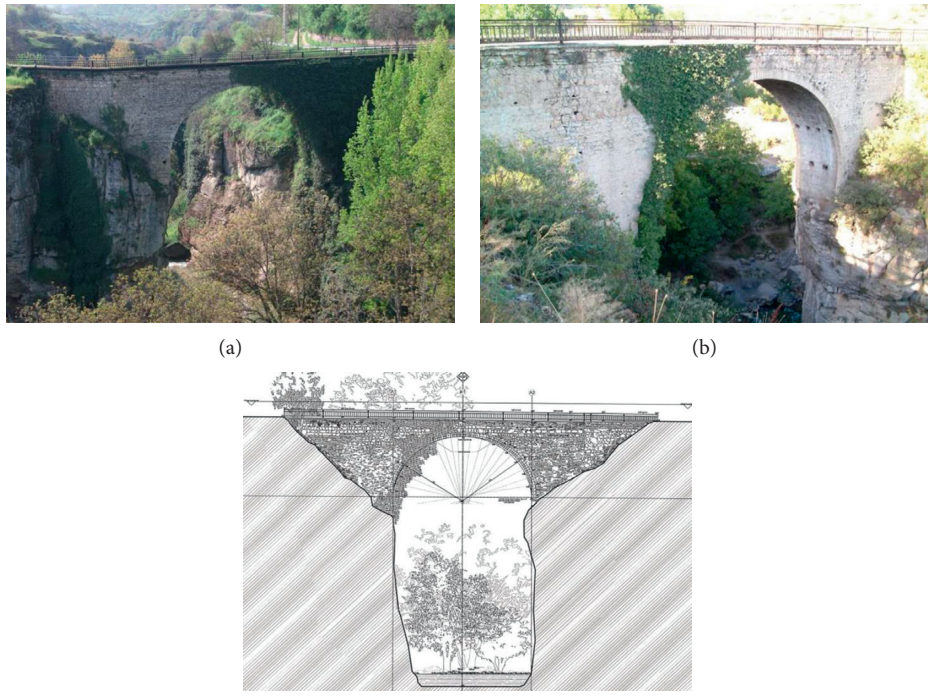

(a) (b)

(c)

Figure 1: View of the historical Tokatlı Bridge: (a) upstream, (b) downstream, and (c) building survey [35].

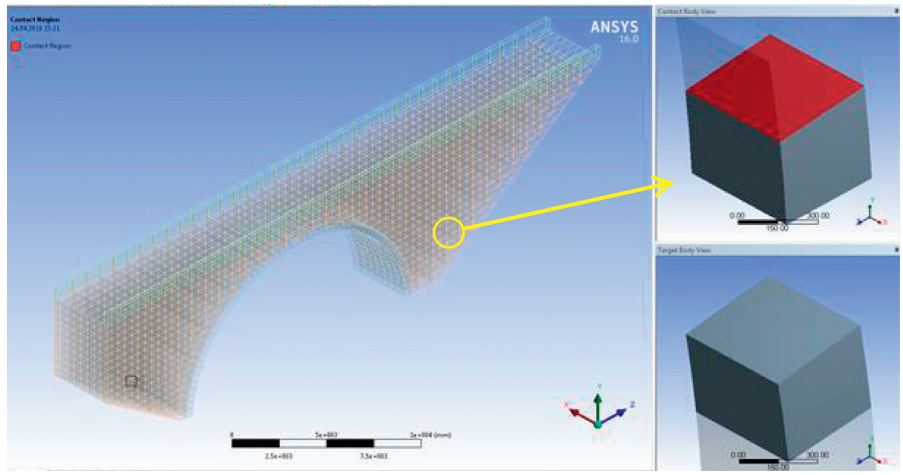

Figure 2: Details of contact surfaces.

conditions is of great importance in FE analysis, as they can greatly affect the structural behavior of the historic Tokatlı Bridge. The boundary conditions are defined by fiefing the translational and rotational degrees of freedom at all bridge abutments and both side walls [1]. Because of the very low tensile strength of the masonry structures, some analytical models and also masonry structure analysis assume that the material model has no tensile strength. The tensile strength value of the wall and the direct tensile bond strength can be determined by flexural bond strength testing. Though the direct tensile bind strength test is problematic to complete, it provides the complete tensile stress-displacement diagram as well as the correct tensile strength [44]. The tensile strength of masonry is usually equal to the tensile bind strength between the joint and the unit [45].

It is known that the compressive strength of the wall in historical masonry bridge elements is much higher than the tensile strength of the wall. The compressive strength of the wall can be viewed as a function of the strength of the bricks and mortar [45]. The basic shape of the stress-strain curve for masonry is shown in Figure 4.

4. Near-Fault Ground Motions

In this study, near-fault ground motions are used due to their distinct, destructive velocity pulse characteristics.

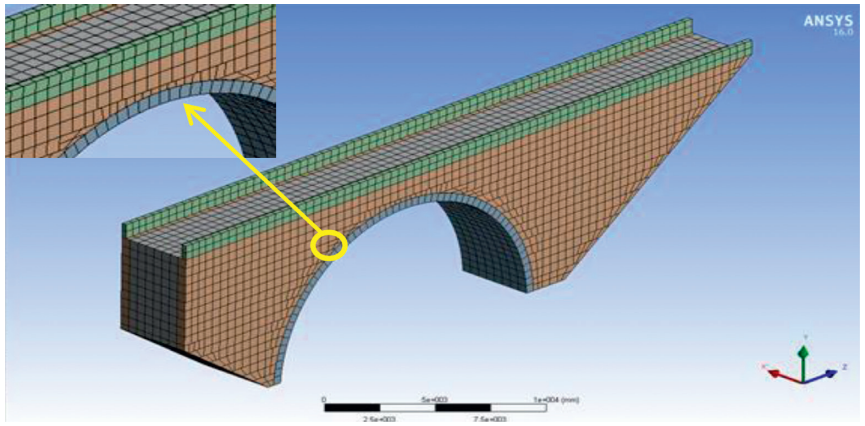

(a)

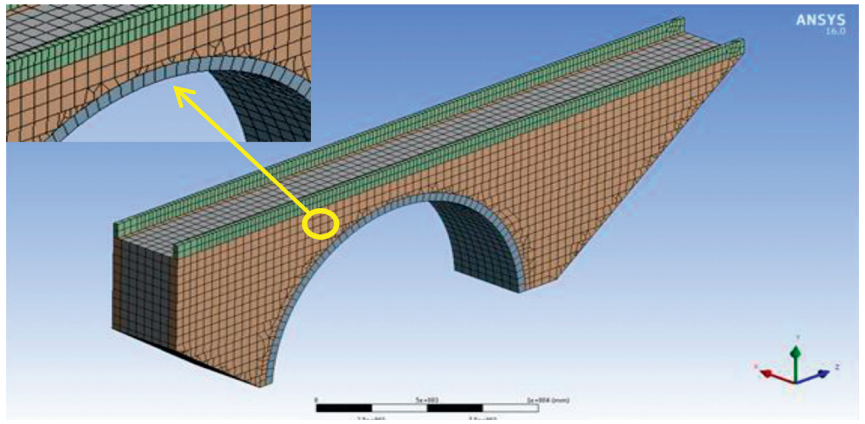

(b)

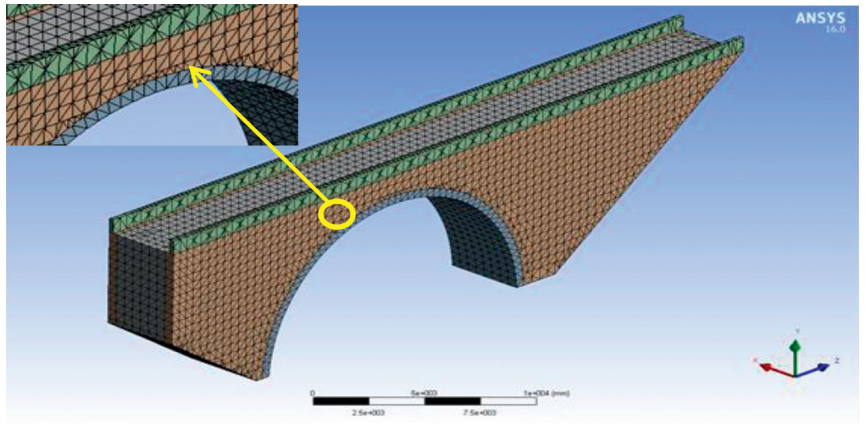

(c)

Figure 3: Mesh options. (a) Hex dominant mesh. (b) Sweep mesh. (c) Tetrahedrons mesh.

Table 1: Numbers of nodes and elements for different mesh types.

Number	Mesh type	Nodes	Elements
1	Automatic	104788	6680
2	Hex dominant	126342	13045
3	Sweep	104788	6680
4	Tetrahedrons	162920	47818

Table 3 lists the near-fault ground motions used in this study. This set of earthquake records used in this study includes near-ground motion parameters, as can be seen in Figure 5. As is known, velocity pulse amplitude (V_p) and velocity pulse period (T_p) are generally used to characterize near-fault ground motions. However, recent research by Makris

Table 2: Material properties [1].

Material	Modulus of elasticity (N/m^2)	Poisson's ratio	Density (kg/m^3)
Stone arches	3.0*E*9	0.25	1600
Timber block	1.5*E*9	0.05	1300
Side walls	2.5*E*9	0.20	1400

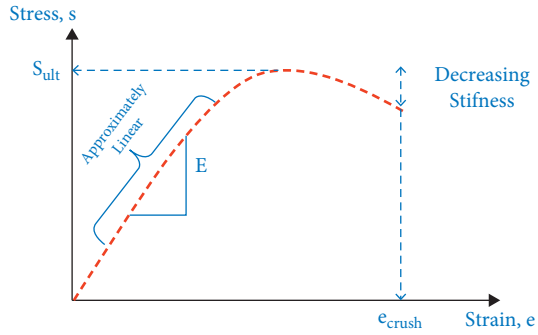

Figure 4: Fundamental stress-strain diagram for masonry under compression [45].

Table 3: Near-fault records used in the analysis.

Earthquake	Station/component	Mag. (Mw)	Distance (km)	A_p (g)	V_p (cm/s)	T_p (s)
Cape Mend. (1992)	89156 Petrolia	7.1	9.5	0.66	90.0	0.7
Kobe (1995)	KOBE/KJM000	6.9	0.6	0.82	81.0	0.9
Superstition Hills (1987)	SUPERST/B-PTS225	6.6	0.7	0.45	112.0	2.2
Northridge (1994)	90056 Newhall-W. Pico Canyon Rd.	6.7	7.1	0.45	92.9	3.2
Imperial Valley (1979)	5165 El Centro diff. Array	6.5	5.3	0.35	71.0	4.5
Chi-Chi (1999)	CHICHI/TCU087-W	7.6	3.2	0.38	120.0	9.5

and Black [40] shows that peak ground acceleration (A_p) appears to be a more significant parameter for characterizing near-fault ground motions [41]. Thus, to characterize the near-fault ground motions considered in this study, both A_p and V_p included within the A_p/V_p ratio of ground motions are used [33]. It is known that this ratio also represents the dominant frequency and energy content of near-fault ground motions [40]. A low ratio indicates ground movements with intense, long-term acceleration pulses, while a high ratio accompanies ground movements with short-term acceleration pulses. One set of ground motions is used. This set involves a suite of 6 earthquakes with distance ranging between 0.6 km and 9.5 km presented in Table 3.

5. Analyses Results

In this phase of the study, the behavior of the historical Tokatlı Bridge under near-fault earthquakes is investigated. For this purpose, as mentioned above, ground motions near the fault are used in this study because of their distinctive, destructive speed-impact properties. Before the dynamic analysis, mode shapes are determined in SAP2000. To obtain the mode shapes and other results, first, a FE model of historical Tokatlı Bridge is determined in SAP2000 as shown in Figure 6. Mode shapes are very important in determining the general behavior of structures. In order to determine the mode shapes, modal analysis was performed in SAP2000 program and the deformation of the first 10 modes of historical Tokatlı Bridge is determined, as shown in Figure 7. Again, the structure of the first 10 mode periods is presented in Table 4. After the creation of the model, dead load analysis is investigated under the bridge's own weight. Maximum deformation, elastic stresses, and stress values obtained as a result of the analysis are shown in Figure 8. To compare the SAP2000 results of historical Tokatlı Bridge under Earth gravity, the ANSYS model is also determined and dead load analysis is also performed under its own weight as shown in Figure 9. As can be seen in Figures 8 and 9, it is observed that pressure stress values are under 20 MPa and tensile stress values are under 1 MPa. Observing the analyses results from SAP2000 and ANSYS under standard Earth gravity, it is seems that stress and displacement values do not cause the collapse of the historical Tokatlı Bridge. While the dynamic behavior under near-fault earthquakes is investigated, stress and displacements graphs are obtained as shown in Figures 10 and 11. Assuming the historical Tokatlı Bridge is stable and undamaged under standard Earth gravity, it can be assumed that there will be no damage to the historical Tokatlı Bridge with the tensile stress increased up to 0.60 MPa. It can be said that this tensile stress obtained is consistent with the tensile strength/compressive strength ratios (1/20–1/10) recommended by Pela et al. [10] for masonry structures, which can be used as a control in assessing the damage potential. Therefore, as mentioned

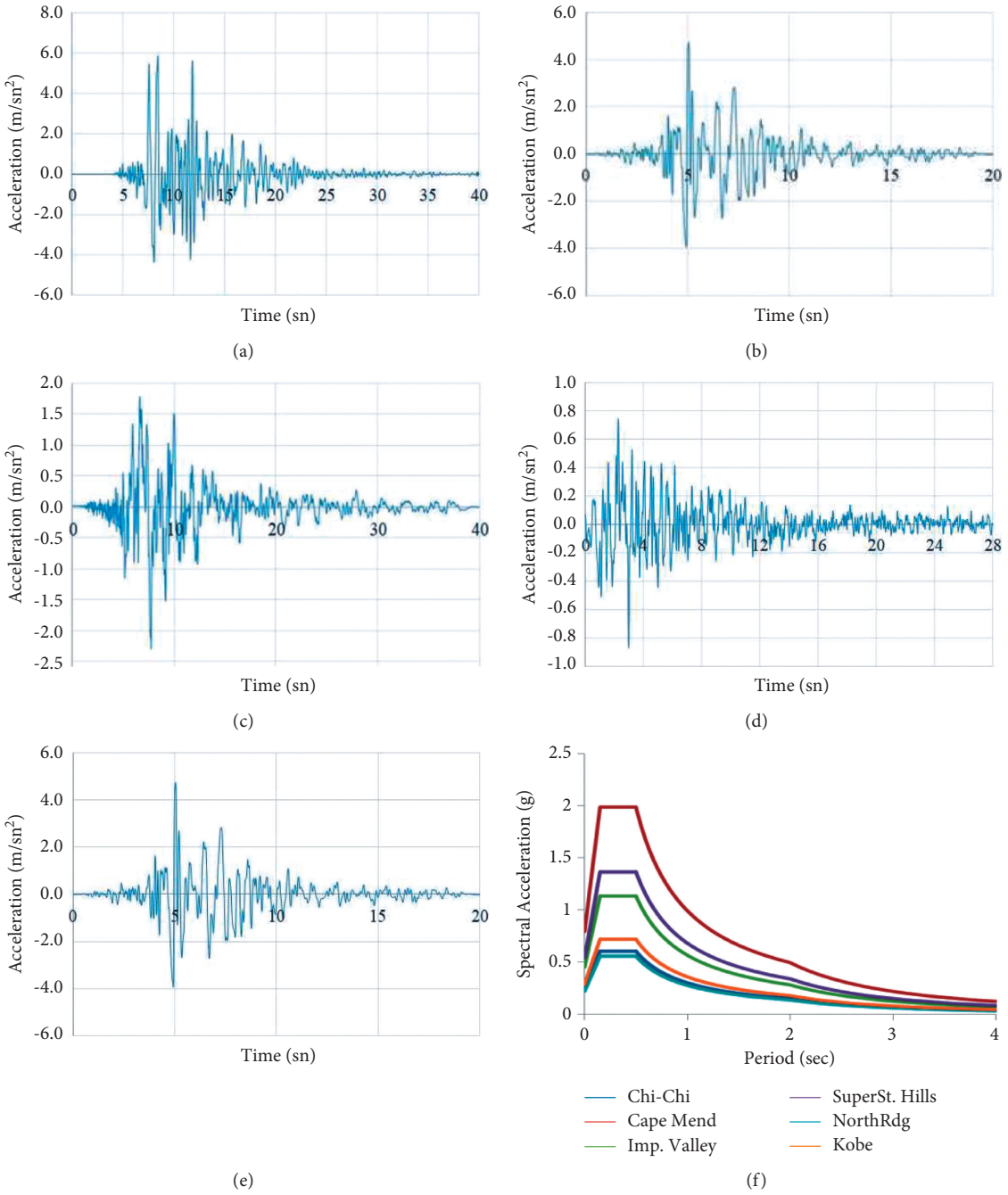

Figure 5: Near-fault earthquakes: (a) Kobe earthquake, (b) Northridge earthquake, (c) Superstation Hill, (d) Imperial Valley earthquake, (d) Cape Mend earthquake, (e) Chi-Chi earthquake, and (f) spectral acceleration response spectrum.

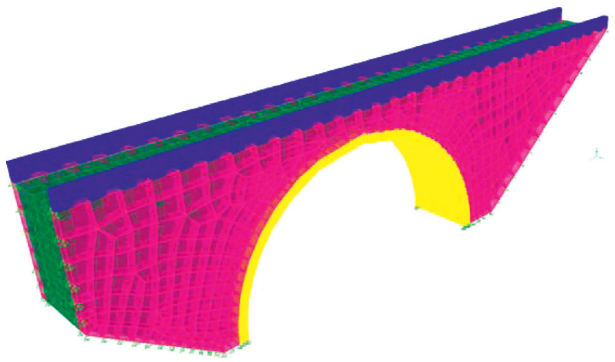

Figure 6: Modeling of historical Tokatlı Bridge in SAP2000.

Table 4: Periods of the first 10 modes of historical Tokatlı Bridge.

Mode	Period (Sn)
1	0.04524
2	0.02531
3	0.02342
4	0.01960
5	0.01656
6	0.01360
7	0.01318
8	0.01296
9	0.01200
10	0.01025

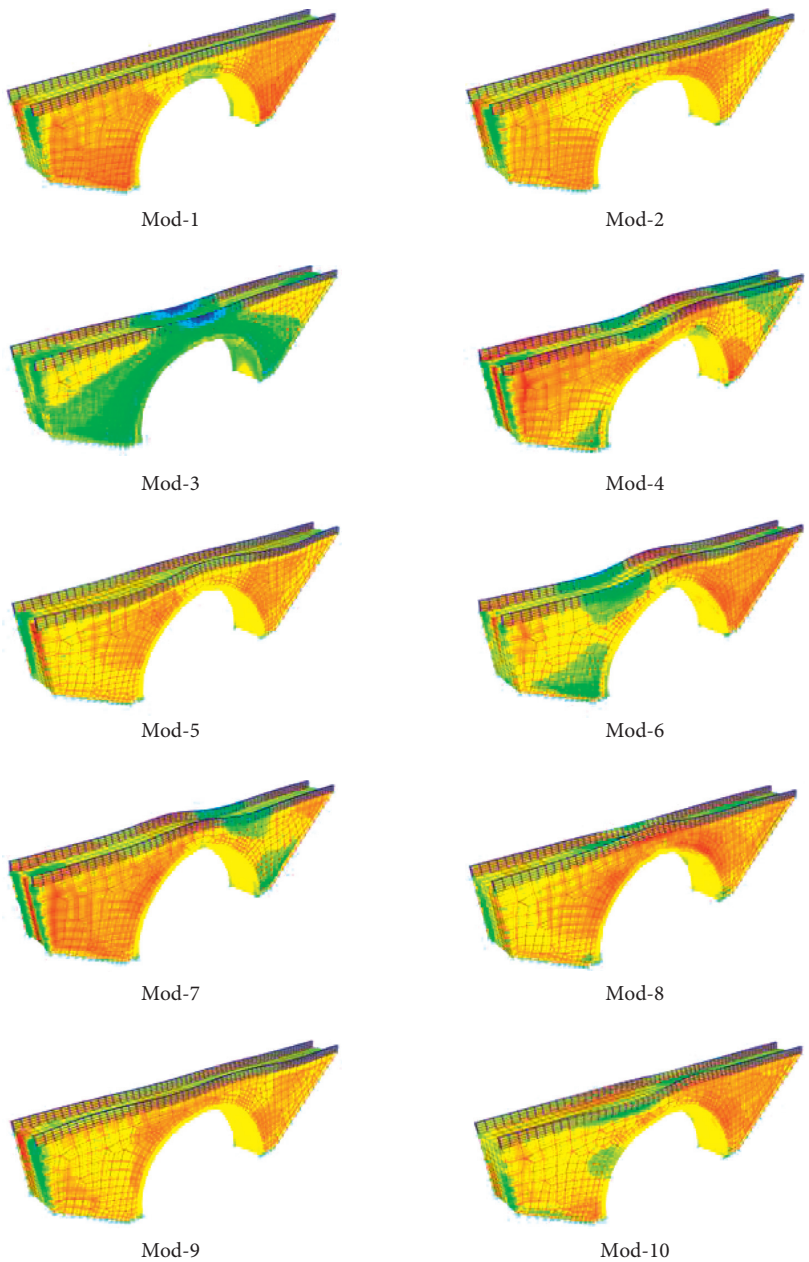

Figure 7: Top 10 mode shapes of Tokatlı Bridge.

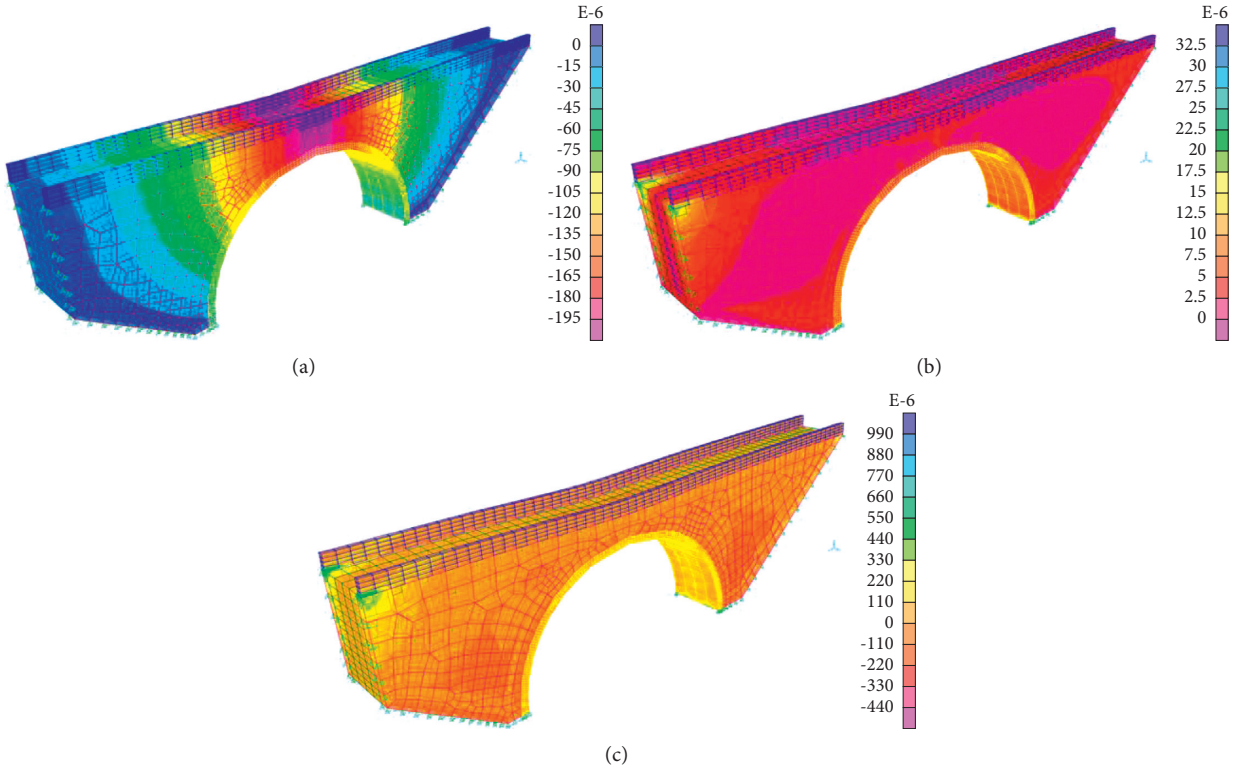

Figure 8: Historical Tokatlı Bridge static analysis in SAP2000: (a) total deformation, (b) maximum principal elastic strain, and (c) maximum principal stress.

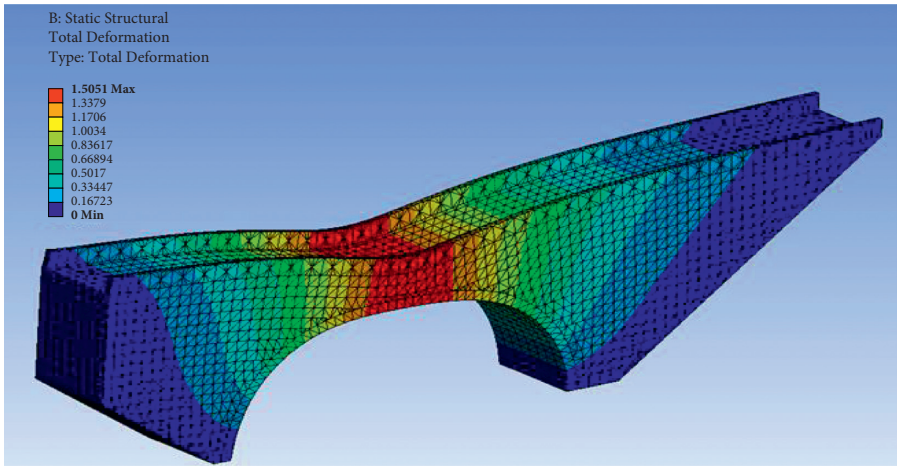

(a)

Figure 9: Continued.

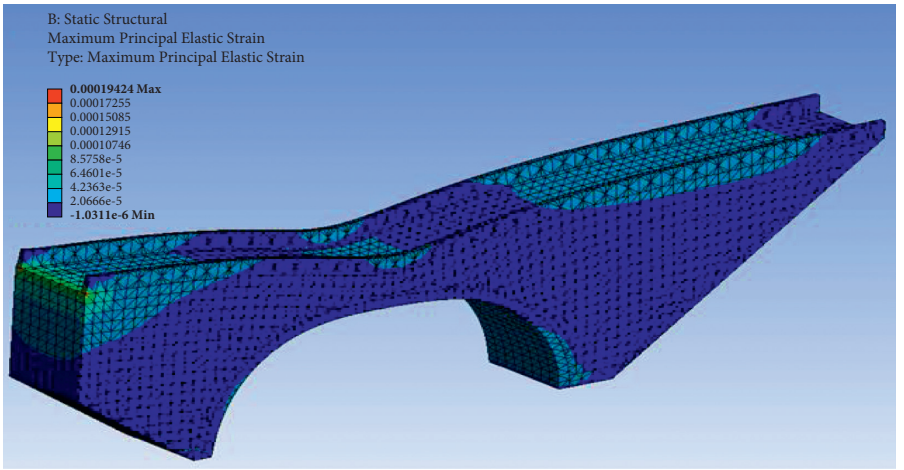

(b)

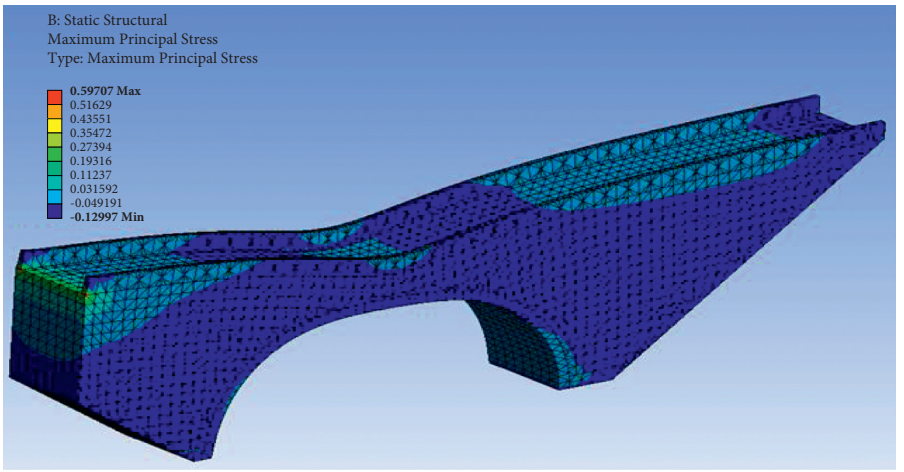

(c)

Figure 9: Historical Tokatlı Bridge static analysis in ANSYS: (a) total deformation, (b) maximum principal elastic strain, and (c) maximum principal stress.

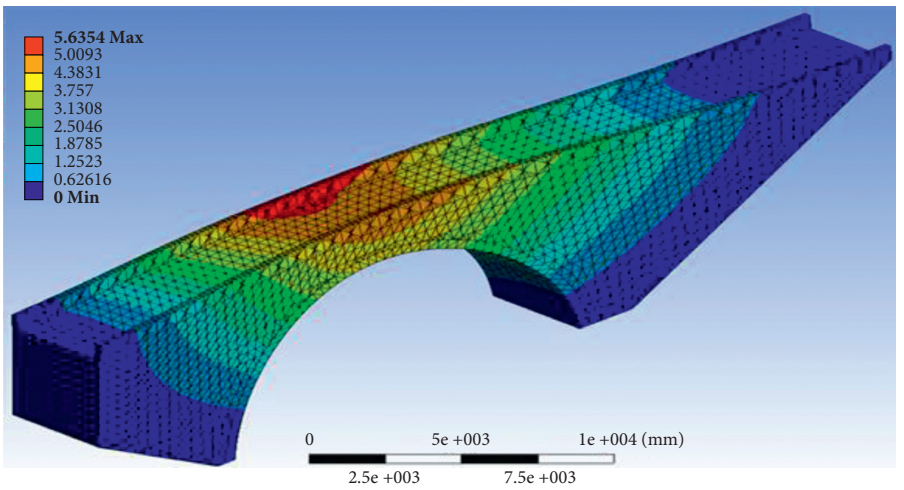

(a)

Figure 10: Continued.

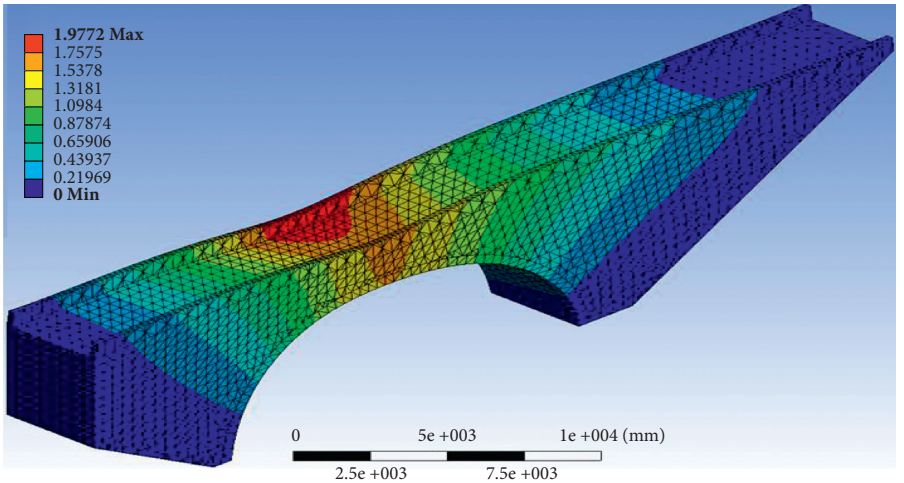

(b)

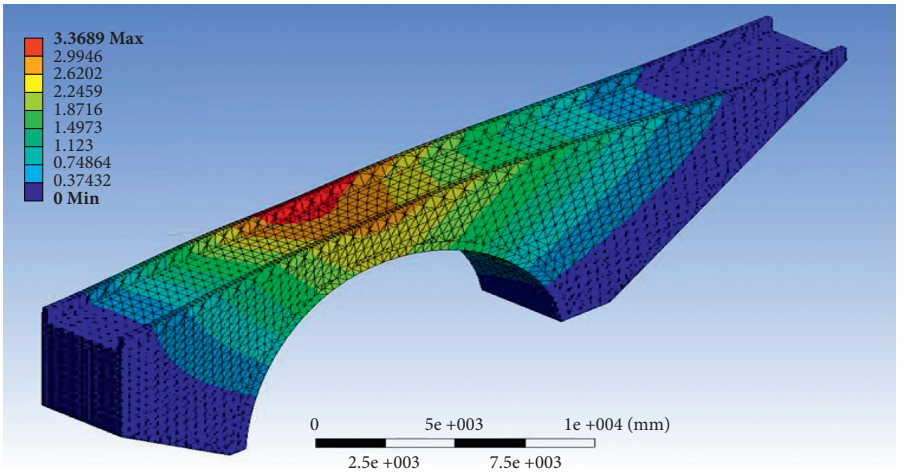

(c)

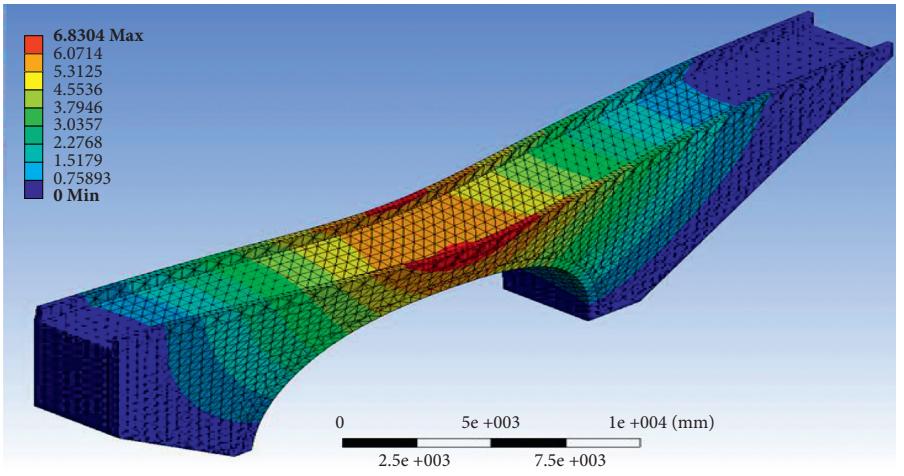

(d)

Figure 10: Continued.

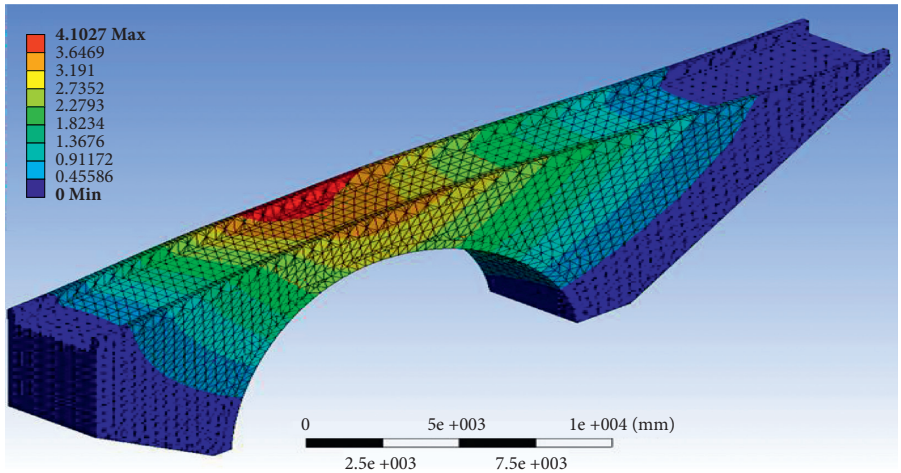

(e)

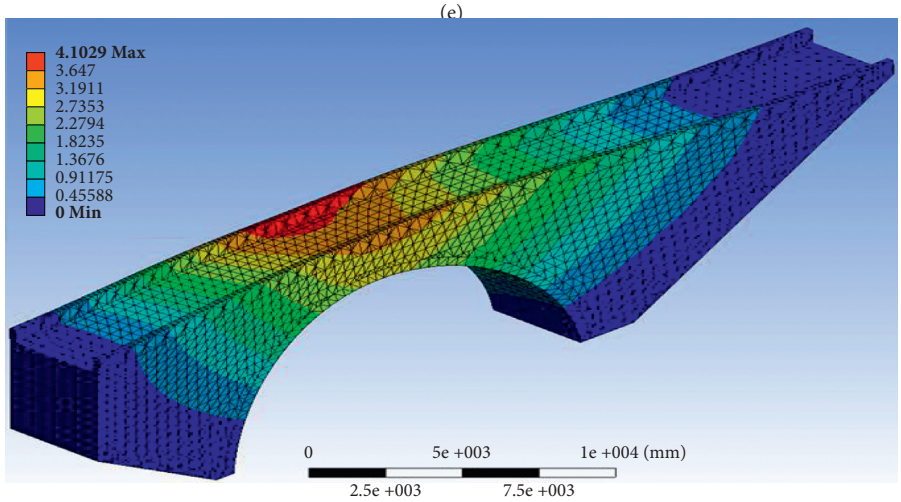

(f)

Figure 10: ANSYS results of historical arch bridge displacements under near-fault earthquakes: (a) Cape Mend earthquake, (b) Chi-Chi earthquake, (c) Imperial Valley earthquake, (d) Kobe earthquake, and (e) Northridge earthquake.

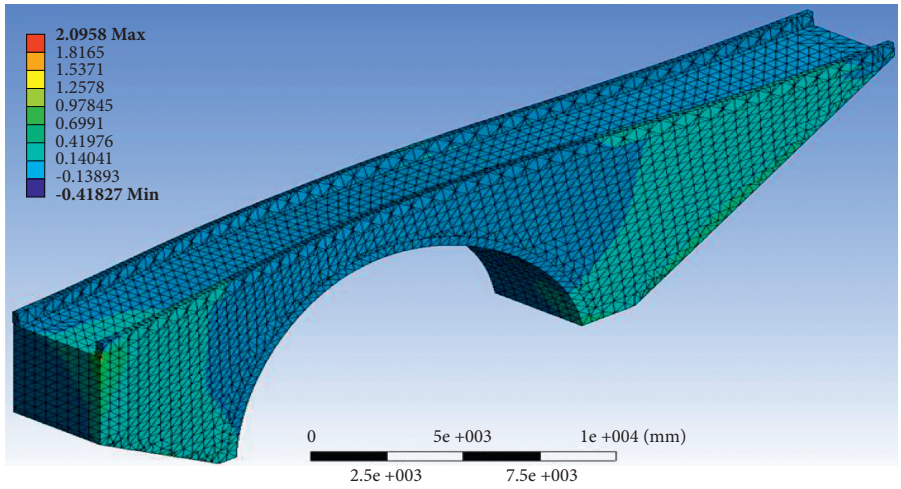

(a)

Figure 11: Continued.

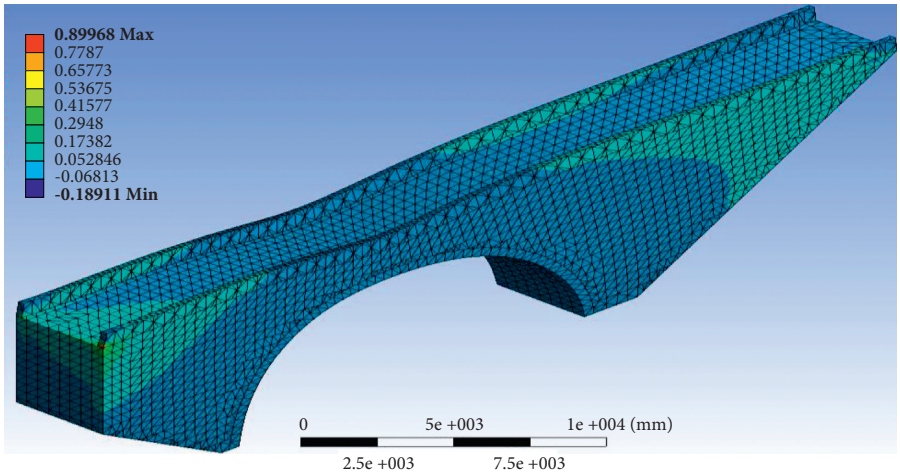

(b)

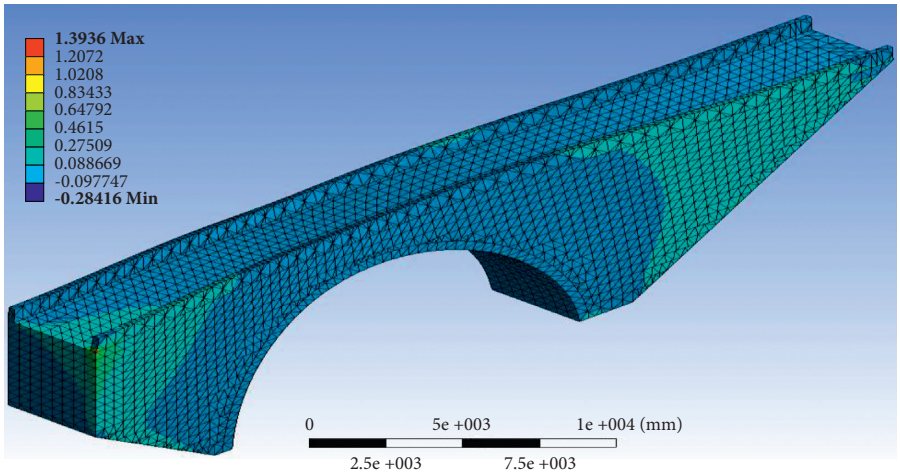

(c)

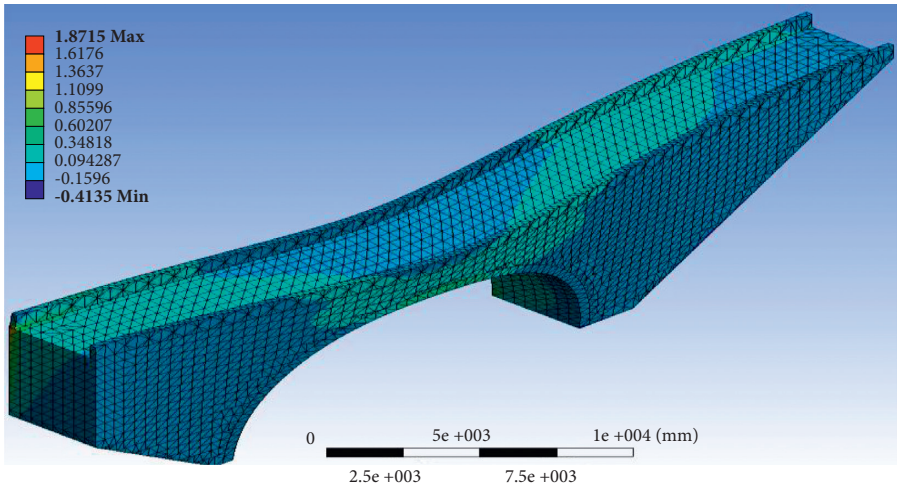

(d)

Figure 11: Continued.

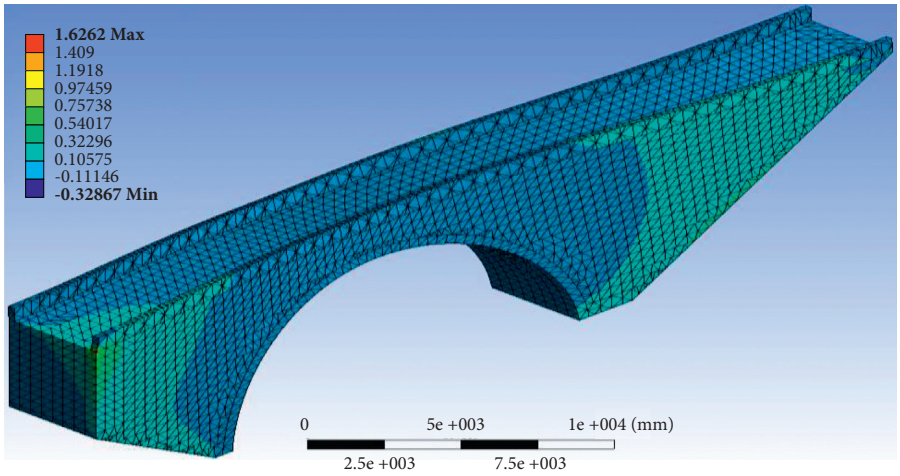

(e)

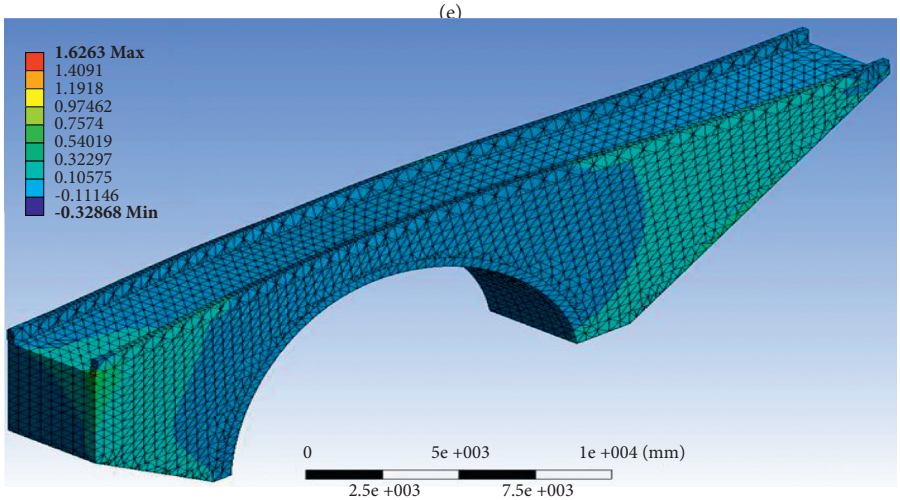

(f)

Figure 11: ANSYS results of historical arch bridge maximum principal stress under near-fault earthquakes: (a) Cape Mend earthquake, (b) Chi-Chi earthquake, (c) Imperial Valley earthquake, (d) Kobe earthquake, and (e) Northridge earthquake.

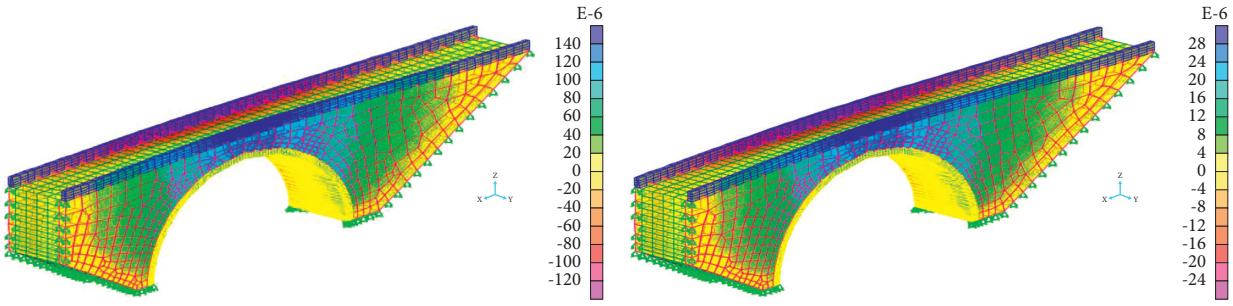

(a) (b)

Figure 12: Continued.

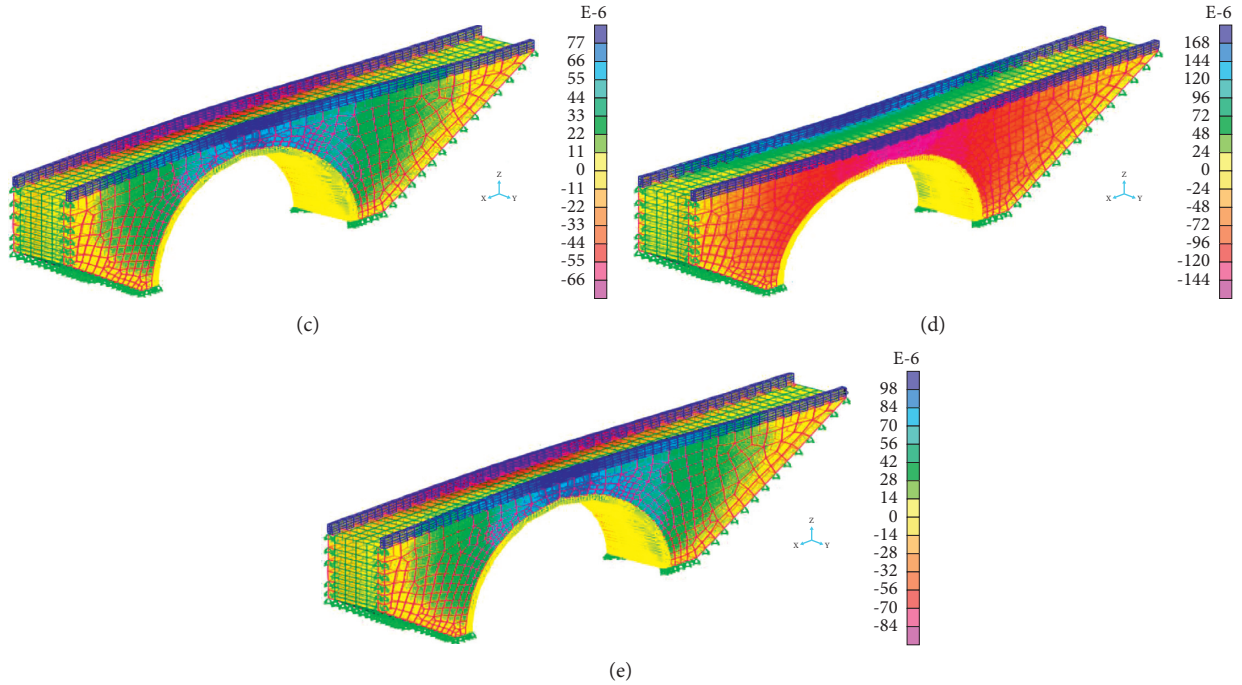

Figure 12: SAP2000 results of historical arch bridge displacements under near-fault earthquakes: (a) Cape Mend earthquake, (b) Chi-Chi earthquake, (c) Imperial Valley earthquake, (d) Kobe earthquake, and (e) Northridge earthquake.

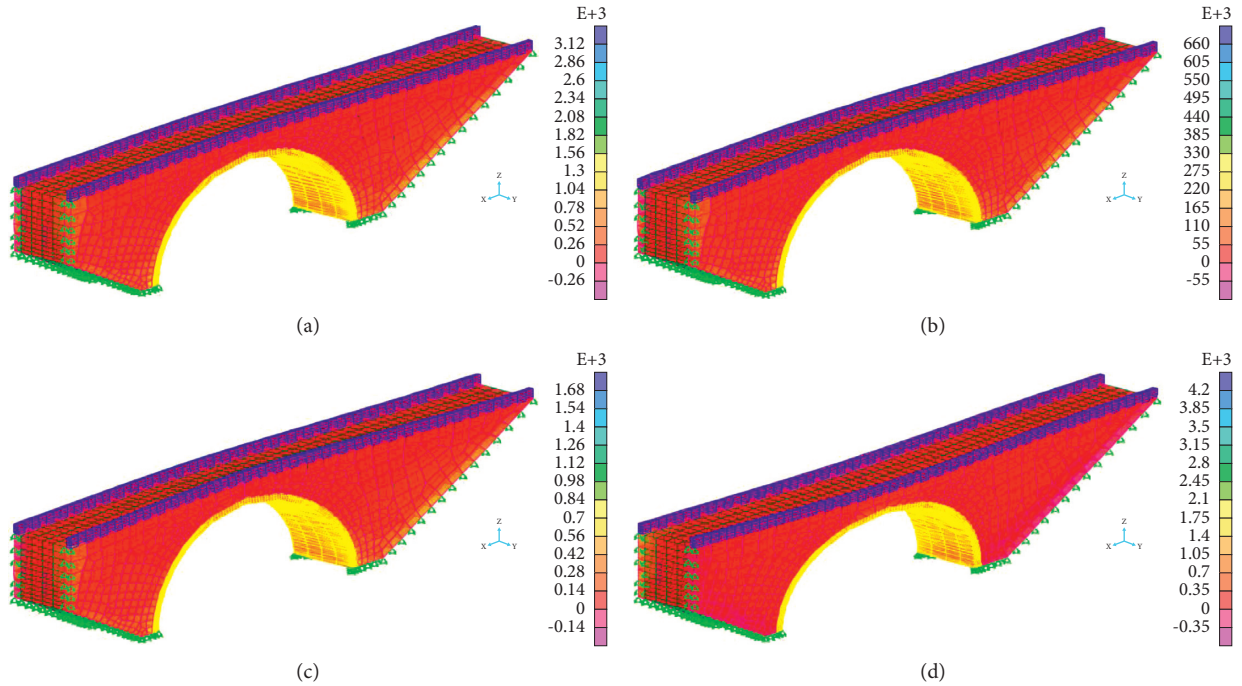

Figure 13: Continued.

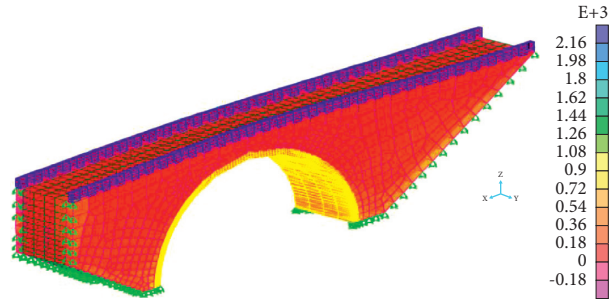

(e)

Figure 13: SAP2000 results of historical arch bridge maximum principal stress under near-fault earthquakes: (a) Cape Mend earthquake, (b) Chi-Chi earthquake, (c) Imperial Valley earthquake, (d) Kobe earthquake, (e) Northridge earthquake.

Table 5: Dynamic ANSYS analysis results.

Number#	Fault	Earthquakes	Historical Tokatlı Bridge		
			Deformation (mm)	Maximum principal elastic strain (mm/mm)	Maximum principal stress (MPa)
1	Near fault	Cape Mend, 1992	5.64	0.00068	2.10
2		Chi-Chi, 1999	1.98	0.00029	0.90
3		Imperial Valley, 1979	3.37	0.00045	1.39
4		Kobe, 1995	6.83	0.00064	1.87
5		Northridge, 1994	4.10	0.00053	1.63
6		Superstition Hills, 1987	4.11	0.00054	1.64

above, in this phase of study, the tensile strength/compressive strength ratio is considered as 1/20 or 5% and the damage potential is evaluated. Therefore, it is predicted that the tensile stress values greater than 1/20 or 5% can be reduced by damaging the structural strength [10]. Furthermore, investigating Figures 10 and 11, it is seen that the tensile stresses increased by the near-fault earthquake effect are more significant especially along the large belt. Considering the near-fault earthquakes loading adopted for the evaluations, the tensile stress reaching up to 0.60 MPa under static loading on the historical Tokatlı Bridge increases up to 2.10 MPa due to the near-fault earthquake effects and exceeds the tensile strength of the historical Tokatlı Bridge which is accepted as 1 MPa. When the finite element model is investigated in detail, it is observed that the tensile stress at many nodes is greater than 1 MPa. These findings indicated that damage may be caused by tensile stress under near-fault earthquakes. As the pressure stresses under near-fault earthquakes effect are quite low than the compressive strength of the historical Tokatlı Bridge, no damage is expected due to pressure. Figures 10 and 11 show that the tensile stress on the historical Tokatlı Bridge surface under near-fault earthquake effects is greater than 1 MPa, which may be risky in terms of damage. As can be seen from Figures 10–13, the upper side of large belt, the bottom of the belt, and the side of the belt can be recommended as critical for damage to the road surface. These findings are consistent with the results in the literature affecting their own weight and earthquake load. In the following stages, cracks that may occur under increasing load effect can be expected to start from these regions and reach the collapse mechanism. Dynamic analysis results are given in Table 5.

6. Conclusions

In this study, a detail investigation about the comparison of static and dynamic behavior of the historical Tokatlı Bridge considering different near-fault earthquakes is presented. For this purpose, a FE model of the historical Tokatlı Bridge is built and analyzed under various near-fault earthquakes using the program ANSYS and SAP2000. Based on the analysis results, the following observations are made:

(i) The maximum displacements decreased when the distance of the earthquakes increased, and this is true for reverse conditions.

(ii) Tensile stresses have reached the permissible masonry tensile strength, especially on the upper side of the large belt, on the upper side of the belt, and on the side of the belt, and pose a risk for damage.

(iii) The compressive stresses are well below the masonry compressive strength and are not considered to be risky in terms of damage. Furthermore, for the historical Tokatlı Bridge, the potential damage due to displacements is found to be critical. However, there is no displacement at the level that would cause damage to the remaining parts of the historical Tokatlı Bridge.

(iv) Contour diagrams obtained as a result of dynamic analysis can be used to determine where damage could potentially occur. Furthermore, the analyses made in this study may be useful for other historical bridges in the country for accurate estimation of responses when considered seismically.

Data Availability

No data were used to support this study.

Conflicts of Interest

The authors declare that they have no conflicts of interest.

References

[1] B. Sevim, A. Bayraktar, A. C. Altunişik, S. Atamtürktür, and F. Birinci, "Assessment of nonlinear seismic performance of a restored historical arch bridge using ambient vibrations," *Nonlinear Dynamics*, vol. 63, no. 4, pp. 755–770, 2011.

[2] C. Ellicks, Ph.D. thesis, The University of Reading, London, UK, 1979.

[3] H. Güllü and M. Karabekmez, "Gaziantep kurtuluş camisinin deprem davranışının i?ncelenmesi," *DÜMF Mühendislik Dergisi*, vol. 7, no. 3, pp. 455–470, 2016.

[4] C. Arnold and R. Reitherman, *Building Configuration and Seismic Design*, Wiley, Hoboken, NJ, USA, 1982.

[5] S. L. Kramer, *Geotechnical Earthquake Engineering*, Prentice-Hall, Hoboken, NJ, USA, 1996.

[6] P. Raychowdhury, "Effect of soil parameter uncertainty on seismic demand of low-rise steel buildings on dense silty sand," *Soil Dynamics and Earthquake Engineering*, vol. 29, no. 10, pp. 1367–1378, 2009.

[7] J. Enrique Luco and A. Lanzi, "Approximate soil-structure interaction analysis by a perturbation approach: the case of stiff soils," *Soil Dynamics and Earthquake Engineering*, vol. 51, pp. 97–110, 2013.

[8] Ö. Emre, T. Y. Duman, S. Olgun, H. Elmacı, and S. Özalp, "Active fault map of Turkey. Ankara (Turkey)," *Bulletin of Earthquake Engineering*, vol. 16, 2012.

[9] F. Mazza and R. Labernarda, "Structural and non-structural intensity measures for the assessment of base-isolated structures subjected to pulse-like near-fault earthquakes," *Soil Dynamics and Earthquake Engineering*, vol. 96, pp. 115–127, 2017.

[10] L. Pelà, A. Aprile, and A. Benedetti, "Seismic assessment of masonry arch bridges," *Engineering Structures*, vol. 31, no. 8, pp. 1777–1788, 2009.

[11] J. Page, *Masonry Arch Bridges—A State of the Art Review*, HMSO, London, UK, 1993.

[12] D. M. Armstrong, A. Sibbald, C. A. Fairfield, and M. C. Forde, "Modal analysis for masonry arch bridge spandrell wall separation identification," *NDT & E International*, vol. 28, no. 6, pp. 377–386, 1995.

[13] A. Bensalem, C. A. Fairfield, and A. Sibbald, "Damping effects on the NDT of soil backfilled arch bridges," *Journal of British Institute NDT*, vol. 40, no. 2, pp. 107–116, 1998.

[14] T. E. Boothby, D. E. Domalik, and V. A. Dalal, "Service load response of masonry arch bridges," *Journal of Structural Engineering*, vol. 124, no. 1, pp. 17–23, 1998.

[15] G. D. Hatzigeorgiou, D. E. Beskos, D. D. Teodorakopoulos, and M. Sfakianaki, "Static and dynamic analysis of the Arta bridge by finite elements," *Archives of Civil Engineering*, vol. 2, no. 1, pp. 41–51, 1999.

[16] P. J. Fanning and T. E. Boothby, "Three-dimensional modelling and full-scale testing of stone arch bridges," *Computers & Structures*, vol. 79, no. 29, pp. 2645–2662, 2001.

[17] G. Frunzio, M. Monaco, and A. Gesualdo, "3D fem analysis of a roman arch bridge," *Historical Constructions*, pp. 591–598, 2001.

[18] S. Toker and A. I. Unay, "Mathematical modelling and finite element analysis of masonry arch bridges," *Journal of Science of Gazi University*, vol. 17, no. 2, pp. 129–139, 2004.

[19] A. Bayraktar, A. C. Altunısık, T. Turker, and B. Sevim, "The model updating of historical masonry bridges using operational modal analysis method," in *Proceedings of the 1st National Conference Reinforcement and Transfer into the Future of Historical Structures*, pp. 429–440, Ankara, Turkey, 2007.

[20] A. Brencich and D. Sabia, "Experimental identification of a multi-span masonry bridge: the Tanaro bridge," *Construction and Building Materials*, vol. 22, no. 10, pp. 2087–2099, 2008.

[21] N. Diamanti, A. Giannopoulos, and M. C. Forde, "Numerical modelling and experimental verification of GPR to investigate ring separation in brick masonry arch bridges," *NDT & E International*, vol. 41, no. 5, pp. 354–363, 2008.

[22] A. Ural, Ş. Oruç, A. Doğangün, and Ö. İ. Tuluk, "Turkish historical arch bridges and their deteriorations and failures," *Engineering Failure Analysis*, vol. 15, no. 1-2, pp. 43–53, 2008.

[23] A. C. Aydin and S. G. Özkaya, "The finite element analysis of collapse loads of single-spanned historic masonry arch bridges (ordu, sarpdere bridge)," *Engineering Failure Analysis*, vol. 84, pp. 131–138, 2018.

[24] A. C. Altunışık, B. Kanbur, A. F. Genç, and E. Kalkan, "Structural response of historical masonry arch bridges under different arch curvature considering soil-structure interaction," *Geomechanics and Engineering*, vol. 18, no. 2, pp. 141–151, 2019.

[25] M. Breccolotti, L. Severinib, N. Cavalagli, F. M. Bonfiglic, and V. Gusellad, "Rapid evaluation of in-plane seismic capacity of masonry arch bridges through limit analysis," *Earthquakes and Structures*, vol. 15, no. 5, pp. 541–553, 2018.

[26] E. N. Rovithis and K. D. Pitilakis, "Seismic assessment and retrofitting measures of a historic stone masonry bridge," *Earthquakes and Structures*, vol. 10, no. 3, pp. 645–667, 2016.

[27] E. Sayin, "Nonlinear seismic response of a masonry arch bridge," *Earthquakes and Structures*, vol. 10, no. 2, pp. 483–494, 2016.

[28] A. Dogangun and H. Sezen, "Seismic vulnerability and preservation of historical masonry monumental structures," *Earthquakes and Structures*, vol. 3, no. 1, pp. 83–95, 2016.

[29] M. Muvafik, "Field investigation and seismic analysis of a historical brick masonry minaret damaged during the Van earthquakes in 2011," *Earthquakes and Structures*, vol. 6, no. 5, pp. 457–472, 2014.

[30] A. Preciado, G. Bartoli, and H. Budelmann, "Fundamental aspects on the seismic vulnerability of ancient masonry towers and retrofitting techniques," *Earthquakes and Structures*, vol. 9, no. 2, pp. 339–352, 2015.

[31] H. Basaran, A. Demir, E. Ercan, H. Nohutçu, E. Hökelekli, and C. Kozanoglu, "Investigation of seismic safety of a masonry minaret using its dynamic characteristics," *Earthquakes and Structures*, vol. 10, no. 3, pp. 523–538, 2016.

[32] F. Cakir, Y. B. Ergen, H. Uysal, and A. Dogangun, "Influence of modified intended use on the seismic behavior of historical himis structures," *Earthquakes and Structures*, vol. 10, no. 4, pp. 893–911, 2016.

[33] M. Karalar, J. E. Padgett, and M. Dicleli, "Parametric analysis of optimum isolator properties for bridges susceptible to near-fault ground motions," *Engineering Structures*, Elsevier Science, vol. 40, , pp. 276–287, 2012.

[34] M. Karalar and M. Yeşil, "Effect of near-fault earthquakes on a historical masonry arch bridge (Konjic Bridge)," *Earthquakes and Structures*, vol. 21, no. 2, pp. 125–136, 2021.

[35] S. Emek, *Karabük Safranbolu Tarihi Aşağı Tokatlı Köprüsü Röleve Restitüsyon Restorasyon Raporu, Karayolları Genel Müdürlüğü 15*, pp. 8–60, Bölge Müdürlüğü, Karabük, Turkey, 2012.
[36] ANSYSANSYS Inc., Canonsburg, PA, USA, 1998.
[37] SAP2000, *Integrated Finite Elements Analysis and Design of Structures*, Computers and Structures, Inc., Berkeley, CA, USA, 2008.
[38] A. K. Jebur, I. A. Khan, and Y. Nath, "Numerical and experimental dynamic contact of rotating spur gear," *Modern Applied Science, Mathematical Models and Methods in Applied Sciences*, vol. 5, no. 2, pp. 254–263, 2011.
[39] B. Yazdızadeh, "Comparison of different plane models in finite element software in structural mechanics," *Proceddings of the Yerevan State Unıversity*, vol. 35, pp. 44–50, 2010.
[40] N. Makris and C. J. Black, "Evaluation of peak ground velocity as a "Good" intensity measure for near-source ground motions," *Journal of Engineering Mechanics*, vol. 130, no. 9, pp. 1032–1044, 2004.
[41] M. M. A. Kadhim, "Factors effect on the effective length in a double strap joint between steel plates and CFRP," *International Journal of Advances in Applied Sciences*, vol. 1, pp. 11–18, 2012.
[42] M. Karalar and M. Yeşil, "Investigation of different arch curvature heights of single-span masonry arch bridge under ground movements," in *Pro8th International Scientific Research Congress - Science and Engineering (UBAK)*, Hattusa, Turkey, August 2020.
[43] M. Karalar and M. Yesil, "Effect of near and far-fault earthquakes on historical Tokatli bridge constructed in Karabük, Turkey," in *ProInternational Congress on Academic Research*, Paris, France, July 2020.
[44] D. V. C. Oliveira, *Experimental and numerical analysis of blocky masonry structures under cyclic loading*, Ph.D. thesis, University of Minho, Department of Civil Engineering, Guimaraes, Portugal and the Structural Technology Laboratory of Universitat Politecnica de Catalunya, Barcelona, Spain, 2003.
[45] G. Ö. Özen, "Comparison of elastic and inelastic behavior of historic masonry structures at the low load levels," Middle East Technical University, Ankara, Turkey, M.S. Master of Science, 2006.